

Mate finding, mating, and population dynamics in a planktonic copepod *Oithona davisae*: There are too few males

Thomas Kiørboe

Danish Institute for Fisheries Research, Kavalergården 6, DK 2920 Charlottenlund, Denmark

Abstract

Three-dimensional (3D) video observations of free-swimming copepods revealed the mechanisms of mate finding in the cyclopoid copepod *Oithona davisae* (cephalothorax length 0.33 mm). The females are ambush feeders and spend almost all of their time sinking slowly through the water, interrupted by 0.5–1-mm-long jumps every few seconds. The sink–jump behavior distributes produced pheromones along an intermittent trail. Males spend about half of their time ambush feeding, and half of their time cruising rapidly (50 body lengths s^{-1}), searching for female signals. On encountering a pheromone patch, the male starts circling rapidly (up to >100 body lengths s^{-1}) around the patch, apparently to find subsequent patches and, eventually, the female. The pursuit may last several tens of seconds, and ends by the male capturing the female or losing the track. Observed reaction distances and male motility patterns were combined with a simple encounter model to estimate a mate-search volume rate of $4.4 L d^{-1}$. The males have a rather limited mating capacity, 0.9 females $male^{-1} d^{-1}$, even when mate-encounter rate is not limiting. Field observations of abundances, combined with estimates of mortality and mate-search and mating capacities, predict that only approximately one-third of the females should be fertilized. This is consistent with field observations, and suggests that population growth in this species is severely constrained by fertilization limitation. Fertilization limitation may apply more generally to populations of pelagic copepods, and may partly account for the frequent observation that female copepods produce sterile eggs, even during periods of a plentiful food supply.

The population dynamics of sexually reproducing zooplankton are governed by variability in fecundity, growth rates, and death rates. The fecundity of pelagic copepods, defined as the production rate of fertile eggs, is often thought of as mainly a function of food availability, food quality, and temperature (Mauchline 1998), but theoretical considerations and circumstantial evidence suggest that it may also be constrained by the capability of the mates to find one another and by the mating capacity of the males (Kiørboe 2006). While the effects of environmental factors on rates of egg production are well documented, both in the laboratory and for field populations (Peterson et al. 1991; Calbet and Agusti 1999; Maps et al. 2005), the significance of fertilization limitation in field populations and the potential implications to the population dynamics have been poorly examined. To my knowledge, there is only one case with direct evidence of fertilization limitation in field populations of copepods (i.e., *Euchaete norvegica*) where the fraction of females fertilized depended on the availability of males (Hopkins 1982; Kiørboe 2006). Yet, there are many reports that significant fractions of mature copepod females in the field either produce nonhatching eggs (Irigoien et al. 2002; Maps et al. 2005) or don't produce eggs at all (Williamson and Butler 1987; Uye and Sano 1995) despite plentiful food

supply and comfortable temperatures. The production of nonhatching eggs is often ascribed to insufficiency or even toxic effects of the food (Ban et al. 1997; Miralto et al. 1999), or to production of resting eggs (Castellani and Lucas 2003), but it is also possible that the eggs are unfertilized (Ianora et al. 1989) and the females unmated since virgin copepod females may produce sterile eggs (Parrish and Wilson 1978; Uchima 1985).

Mate finding represents a particular challenge to small zooplankters living in a three-dimensional (3D) world where the distance to the nearest mate may be substantial, but most species of pelagic copepods have behaviors that enhance mate-encounter rates (Doall et al. 1998; Tsuda and Miller 1998; Bagøien and Kiørboe 2005). Often the mates are capable of remotely detecting one another using either hydromechanical or chemical signals, and typically the males have developed swimming patterns that optimize the chance of finding a female signal. Signal extension and motility patterns have been quantitatively described in a handful of calanoid copepods and incorporated in simple mechanistic models that have allowed estimation of mate-search and encounter rates (Kiørboe and Bagøien 2005). These models have led to a theoretical understanding of the possible constraints of the mating biology on the population dynamics (Kiørboe 2006). The prediction of these theoretical considerations is that mate-encounter and male mating capacity at times may leave a substantial fraction of the population unfertilized and that this may limit population growth. However, good empirical evidence and observations that directly link the small-scale behavior of the individuals to properties of the population are lacking.

This study quantitatively examines the mating biology of a small cyclopoid copepod, *Oithona davisae*, and integrates

Acknowledgments

This study received financial support from the Danish Natural Research Council and the Spanish Ministry of Education and Science. I thank Enric Saiz and the zooplankton ecology group at Institut de Ciències del Mar, Barcelona, for support and stimulating discussions, Juancho Movilla for technical assistance, Shin-Ichi Uye for sharing data, and Kasper Kristensen for help with statistical analysis.

observations of the individual behaviors to make predictions about the population. These predictions, in turn, are tested against field observations provided by Uye and Sano (1995, 1998). Qualitative observations in a dissecting microscope (Uchima and Hirano 1988; Uchima and Murano 1988) have previously been used to describe the swimming and mating behavior of this species, and these observations have suggested that the females produce pheromones to signal their presence and position to potential males. Here, I reexamine and quantify the mating behavior in *O. davisae* using simple mating experiments and 3D video observations of freely swimming animals. I show that the characteristics of the individual mating behavior can account quantitatively for the seasonal variation in the (high) fraction of nonbreeding females in the field population observed by Uye and Sano (1995), thus demonstrating that the population dynamics are severely constrained by mating limitation.

Materials and methods

O. davisae were grown in continuous cultures at the Institut de Ciències del Mar, Barcelona, Spain, where all experiments and observations were also conducted. The cultures were fed *Oxhyrris marina*, which, in turn, was grown on *Rhodomonas salinas*. Cohorts were produced from recently hatched eggs to get experimental animals of uniform age that had matured within a few days. Late copepodite stages were isolated individually in 2-mL Nunc Well Multidishes where they were fed and kept until maturation (near 100% survival). All experiments were conducted at 20–22°C in darkness (except for infrared light for filming) and with food offered at saturating concentrations. Cephalothoracic lengths of experimental animals averaged 0.30 mm (males) and 0.34 mm (females), and males had an antennal span of 0.40 mm.

To quantify sex-specific motility patterns in two dimensions (2D), 10–20 males or females were added to an 8 × 8 × 8 cm cubic plastic aquarium. The densities of copepods in these and subsequent experiments were all well within the range of adult densities observed in nature (e.g., Uye and Sano 1998). Collimated infrared light from a light-emitting diode (LED) was provided from the back, and shadow images of the copepods were video recorded from the front with a black-and-white charge-coupled device (CCD) equipped with a 35-mm lens. The frame rate of the CCD was 25 Hz. Sequences of 3–4-min duration were stored directly on a computer, and 2D projections of swim tracks were digitized using LabTrack software (BIORAS) as described by Kjørboe and Bagøien (2005). More than 100 swim tracks, combined from several experiments, were analyzed for each sex (109 female, 296 males). Population motility patterns were analyzed by plotting the root-mean-square (RMS) net distance traveled as a function of time (t). The $\text{RMS}(t)$ was computed as:

$$\text{RMS}(t) = \left[\frac{1}{n} \sum_{i=1}^n \{ (x(i,0) - x(i,t))^2 + (y(i,0) - y(i,t))^2 \} \right]^{1/2},$$

where n is the number of tracks analyzed and $x(i,0)$, $y(i,0)$

and $x(i,t)$, $y(i,t)$ are the (x,y) positions of the i th track at its start and at time (t) after its start.

For a perfect random walk (diffusive motility), the RMS distance increases with the square root of time. However, if the motility has some directional persistence, then at small temporal and spatial scales, the RMS distance will increase in proportion to time (ballistic motility). The transition between ballistic and diffusive motility occurs at a characteristic scale, the motility length scale, which can be estimated from the plot of RMS net distance versus time (see Kjørboe and Bagøien 2005; Visser and Kjørboe 2006). Mate-encounter rates depend on the magnitude of the motility length scale relative to the size of the target (e.g., the spatial extension of the female signal), and it is most efficient when the former exceeds the latter.

Mate-finding behavior and 3D swimming tracks were examined in 5 × 5 × 5 cm cubic aquariums. Relative to the size (weight) of the copepods, these aquariums were similar in size to the aquariums used in previous copepod mating studies (e.g., Doall et al. 1998; Tsuda and Miller 1998; Bagøien and Kjørboe 2005). Each aquarium was equipped with a diagonally positioned mirror. Collimated infrared light was provided from one side, and swimming copepods and their mirror images were video recorded through the perpendicular side of the aquarium. In eight mate-finding experiments, approximately five males and five females were added to the aquarium, and recordings were continued for 1–3 h. 3D swimming tracks of selected individuals were reconstructed by combining the time-varying positions of individual copepods and their mirror images using ImageJ software. 3D animations of mate searches, encounters, and pursuits were made in MatLab (MathWorks, Inc., Natick, Massachusetts) or ImageJ (<http://rsb.nih.gov/ij/>). The 3D reconstructions were also used to estimate all distances and velocities. Many mating events were observed, and for nine of these, male and female swimming tracks were digitized 0.5–2 min prior to the male grasping the female.

To examine the mating capacity of males (i.e., how many females a male can fertilize per unit time), three or four males were incubated on two occasions together with >30 virgin females and plenty of food in ~25 mL of water for 2 or 3 d. At this female density, mating rate is not limited by mate-encounter rate. One to two times per day, females with egg sacs were removed and transferred individually to 2-mL multidishes, and the fate of the eggs (hatching or not) was examined 2–3 d later. Successful mating events were modeled as a Poisson process, and mating rate and confidence interval were estimated by the maximum likelihood method (General Linear Model with Poisson distributed response variable).

Results

Swimming behavior and motility patterns—The females are ambush feeders and spend most of their time motionless while sinking slowly through the water at 0.1–0.3 mm s⁻¹, only interrupted by jumps every 2–5 s (Fig. 1; Table 1). Jump distances are up to 0.5–1 mm (Fig. 1B), most often

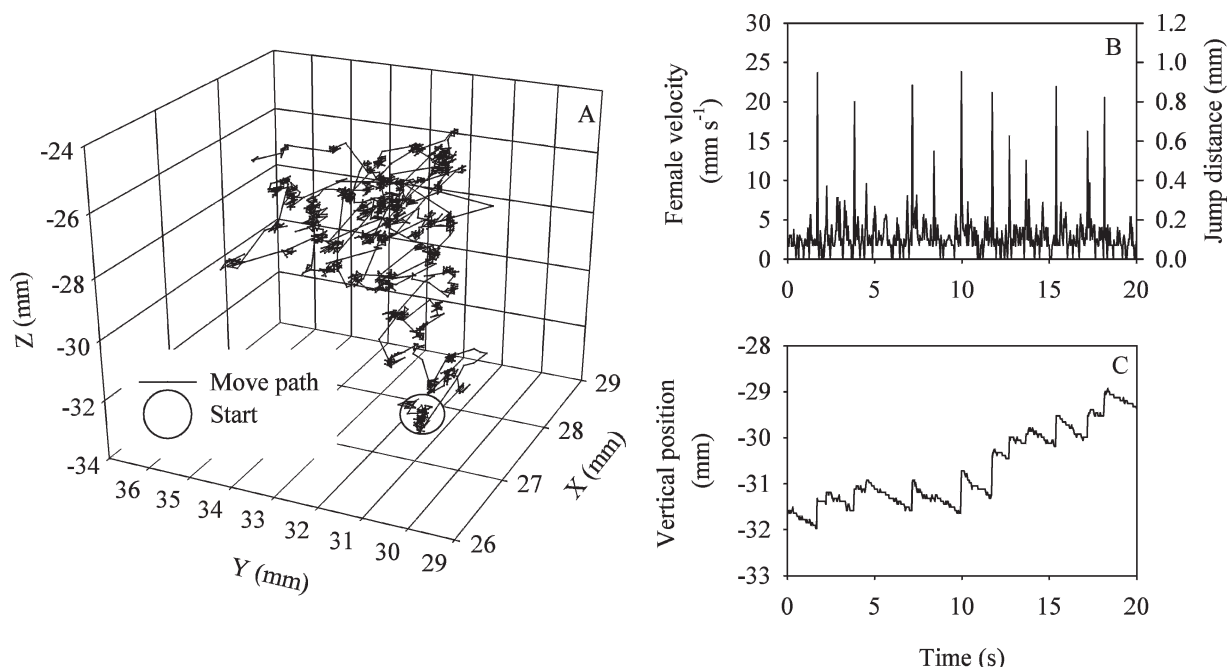


Fig. 1. (A) 3D movement pattern of an ambush feeding female *O. davisae* followed for ~1.5 min with its position digitized at 25 Hz. (B) Velocity and jump distances of the female and (C) its vertical position during a 20-s period.

upward. Motile prey, in this case *O. marina*, are perceived and captured individually. This general motility pattern is only interrupted very occasionally in undisturbed females, e.g., by longer (up to 5–10 mm) escape-like jumps or by a series of jumps. Analyses of multiple swim tracks in 2D reveal that the female motility is almost purely diffusive and with very little directional persistency (motility length

scale ~0.1 mm) (Fig. 2A,B). The estimated average propagation velocity was $0.5 \pm 0.6 \text{ mm s}^{-1}$, which is the net result of sinking and jumps.

Male motility patterns are entirely different from those of the females, primarily because the males spend a substantial fraction of their time swimming at high velocity (Fig. 2C,D). In the absence of females, the males cruise at

Table 1. Characteristics of female motility as well as response distance, along-trail distance to female, and trail age at point of response for nine digitized mate-encounter events in *O. davisae*. For some events (Nos. 14, 17, 18, and 22), the male lost and found the female signal, and response and trail distances and ages have been given for each signal encounter.

Event No.	Jump frequency (s ⁻¹)	Sinking velocity (mm s ⁻¹)	Response distance (mm)	Along-trail distance (mm)	Trail age at point of response (s)	Corrected along-trail distance* (mm)
4	0.57	0.29	3.9	6.5	7.6	4.3
11	0.29	–	10.0	12.0	18.8	9.3
13	0.25	–	2.8	4.7	12.2	3.2
14	0.18	–	1.4	1.4	–	–
			1.4	1.3	4.0	0.9
17	0.39	0.1–0.25	2.0	–	–	–
			1.0	2.3	4.3	1.5
			2.4	4.0	5.8	2.9
18	0.26	0.16–0.30	5.0	11.2	23.8	8.1
			1.7	0.7	1.9	0.5
19	0.27	0.099	1.9	3.4	10.1	2
22	0.25	0.13	4.0	–	–	–
			10.3	21.2	42.6	15.9
23	0.2	0.08	–	–	–	–
Average ± SD	0.28 ± 0.12	0.17 ± 0.08	3.7 ± 3.1	6.2 ± 6.2	13.1 ± 12.4	4.9 ± 4.9

* Corrected along-trail distance = along-trail distance – (jump frequency × trail age × jump length) and is computed from an average jump distance of 0.5 mm and event-specific jump frequencies and trail ages (see text for further explanation).

* Corrected along-trail distance = along-trail distance – (jump frequency × trail age × jump length), computed from an average jump distance of 0.5 mm and event-specific jump frequencies and trail ages (see text for further explanation).

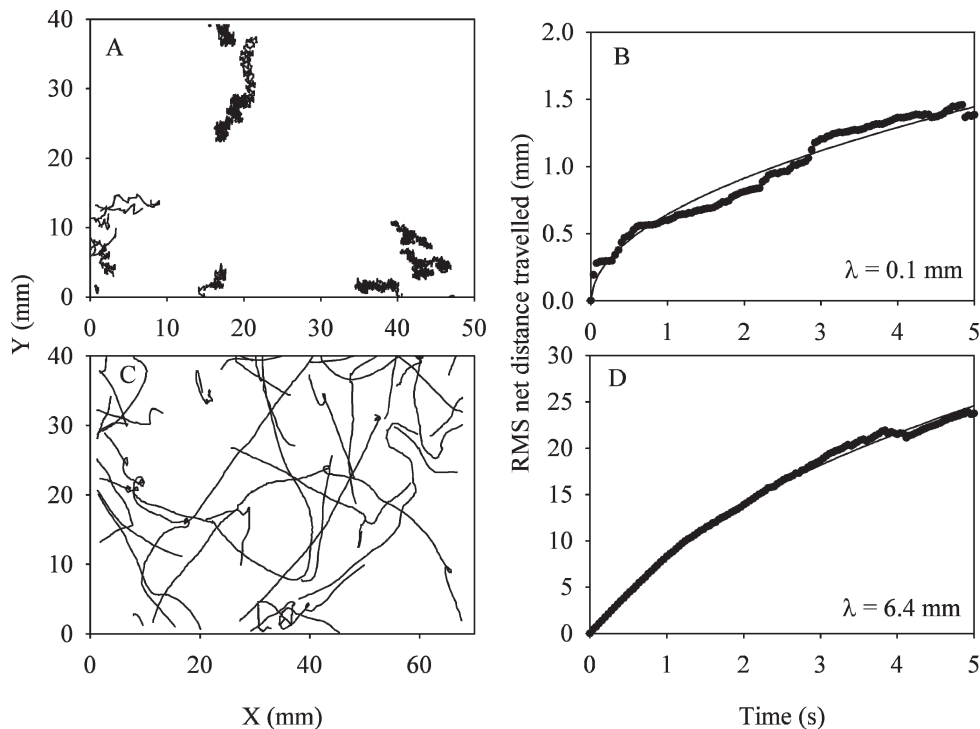


Fig. 2. 2D projections of move tracks of (A) female and (C) male *O. davisae* and plots of root-mean-square distance traveled as a function of time for populations of (B) females and (D) males. Solid lines in panels B and D are fits of Taylor's equation (Visser and Kjørboe 2006); the estimated motility length scales (λ) have been given. All data are based on observations of virgin adults and in the absence of the opposite sex.

a velocity of about 15 mm s^{-1} , corresponding to about 50 body lengths s^{-1} , and along relatively straight lines. The estimated motility length scale is 6.5 mm, and the motility pattern of the males, thus, has a strong directionality and is nearly ballistic at spatial scales $< 6.5 \text{ mm}$.

Qualitative inspection of Fig. 2C overemphasizes the importance of fast-moving males, but in fact many males at any point in time are ambush feeding in a manner similar to the females. One can do an approximate time budget by analyzing the frequency distribution of swimming velocities (Fig. 3). The bimodal distribution of swimming velocities, most clearly seen for the males, reflects the two motility types, ambush feeding (slowly sinking) and swimming or jumping. For females, slowly sinking accounts for 97% of the observations (i.e., the females are feeding 97% of the time). For the males, sinking takes up to 48% of the time (i.e., a substantial fraction of time is spent feeding, even in males). The grand average swimming velocity of males is $7.9 \pm 8.2 \text{ mm s}^{-1}$, but the average velocity of those that actually swim is $15.0 \pm 6.0 \text{ mm s}^{-1}$.

Mate finding—Males expand their behavioral repertoire in the presence of females. In addition to cruising and feeding they may intermittently swim at very high velocities (up to $> 40 \text{ mm s}^{-1}$ or > 100 body lengths s^{-1}) in a spiraling or circling pattern (Fig. 4; see video and animation in Web Appendix 1, http://www.aslo.org/lo/toc/vol_52/issue_4/

[1511a1.html](#)). Swimming velocity varies substantially: for the male shown in Fig. 4, cruising occurred at a modest velocity of $\sim 10 \text{ mm s}^{-1}$ (Fig. 4A,B) and small-scale circling (diameter of circles $< 1 \text{ mm}$) at an intermediate velocity (Fig. 4A,C), whereas the highest velocities were associated with larger-scale circling (diameter 5–10 mm; Fig. 4D,E). The velocity estimates are conservative since corners are cut when the copepod turns frequently and its position is digitized only at 25 Hz. High-speed circling behavior is likely a response to a chemical signal (pheromone) produced by the females and elicited when a male encounters a female scent patch. Mate encounters were in all cases preceded by circling behavior, but in the small experimental aquariums with high densities of females, circling behavior often occurred apparently unrelated to any particular females.

In several cases, circling behavior was directed toward a particular female and constituted what looked like female pursuit that concluded with the male catching the female. I observed many mate encounters and catches, nine of which were digitized and analyzed in detail (Table 1). An example of a typical signal encounter, pursuit, and catch is illustrated in Figs. 5 and 6 and occurred as follows: a male cruising at $\sim 10 \text{ mm s}^{-1}$ comes into the vicinity of a female (Fig. 5B); at a distance of 4 mm from the female, the male appears to encounter a signal (at time 36:20 s), accelerates to $\sim 30 \text{ mm s}^{-1}$ (Fig. 6A), and starts fine-scale circling a few millimeters away from the track of the female (Fig. 5C).

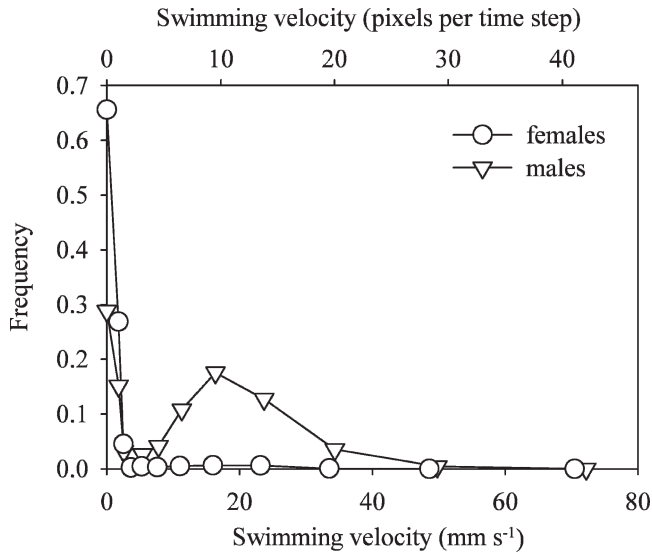


Fig. 3. Swimming velocity frequency distribution of virgin male and female *O. davisae* in the absence of the opposite sex ($n = 49,000$ for males and $53,000$ for females). Swimming velocities have been reported both in units of mm s^{-1} (lower x -axis) and units of pixels per time step (upper x -axis).

After a few seconds, he apparently loses the track and then engages in large-scale circling, still at a very high velocity ($>20 \text{ mm s}^{-1}$, Fig. 5D). He finds the signal of the female again at time 51:08 s and resumes fine-scale circling around her track (Fig. 5E). This second response to the signal occurs at a distance of 10.3 mm from the female. The female was at this position more than 40 s earlier, and her swimming distance during these 40 s was 21 mm (along-track distance). Meanwhile, the female continues her jump-and-sink feeding apparently unaffected. Eventually, the male strikes at the female from a distance of ~ 2 mm, which elicits an escape jump from the female. The final chase (from ~ 58 s onwards; Fig. 5F) consists of a series of strikes and female escapes until eventually the male catches the female. 3D animations of similar events are available in Web Appendix 1.

All the events observed blended the different components of the pursuit differently, but otherwise followed a similar pattern, where the male may find, lose, and again find the signal of the female several times before the pursuit is concluded with either capture or permanent loss of the female signal. Response distances varied between 1 mm and 10 mm, and distances measured along the swimming track of the female were between 1 mm and 21 mm (Table 1). The age of the female track at the point of response was up to 43 s (Table 1). Fresh trails were more often encountered than older trails, and there was an inverse relation between encounter frequency and the along-trail distance (Fig. 7).

Mating capacity—The cumulative number of fertilized females (i.e., females with eggs that hatch) per male increased linearly with time (Fig. 8A). The male mating capacity was 0.9 successful matings $\text{male}^{-1} \text{d}^{-1}$ (95% confidence interval: 0.5–1.4 matings per male and day).

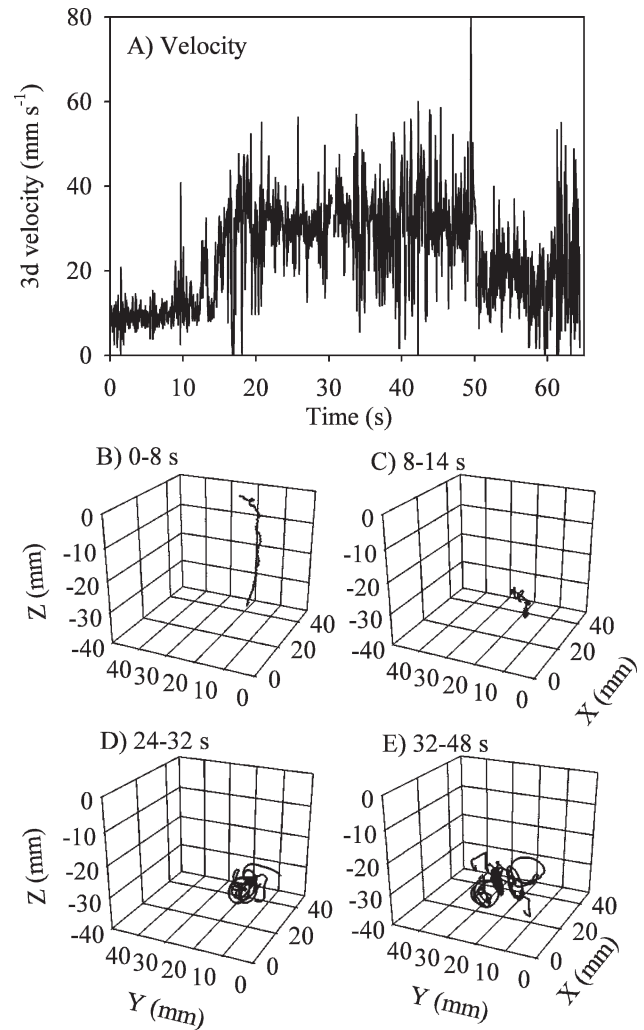


Fig. 4. (A) Swimming velocity fluctuations and (B) 3D move track of a male *O. davisae* followed for ~ 1 min.

Some females produced eggs that did not hatch (Fig. 8B); these were considered unfertilized. These females kept the eggs for at least a week. The fraction of unfertilized females carrying eggs increased at a rate of 0.09 d^{-1} (Fig. 8B). Mated females always carried two spermatophores that are deposited during one mating event (verified by checking females immediately after first mating).

Discussion

The mate-finding behavior observed here is largely consistent with the description provided by Uchima and Murano (1988) based on observations of copepods in a petri dish but adds insights that can only be revealed from the 3D observations (e.g., swimming speeds and reaction distances) and that allow a more detailed interpretation. In the following, I first interpret the observations to reveal the mechanisms of mate finding, then use this interpretation to quantify mate-search capacity, and, finally, I examine the population-dynamics consequence of the observed behavior.

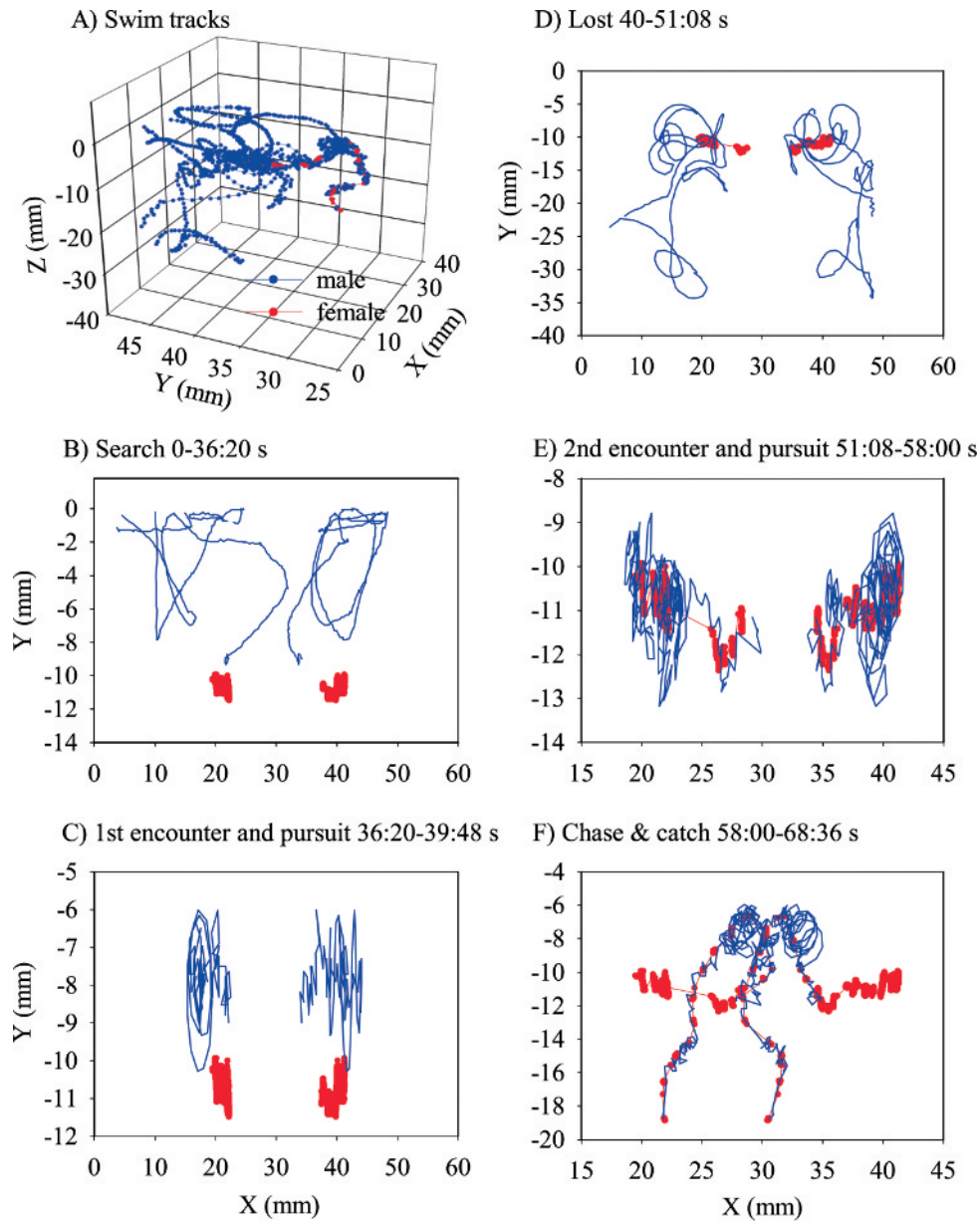


Fig. 5. (A) 3D swim tracks of male and female *O. davisae* during mate search and encounter and (B–F) the same event split up in sequences of (B, D) search, (C, E) encounter and pursuit, and (F) chase and mate catch. Panels B–F show 2D projections of male (blue) and female (red) swim tracks of both the copepods (left part in each panel) and of their mirror images (right).

Character and extension of the female signal—Obviously, the female signals her presence and position to the male, and the signal must primarily be of chemical rather than of hydromechanical nature. Hydromechanical signals generated by the occasionally jumping females can be detected only at distances up to a few millimeters, which is inconsistent with detection distances of >10 mm. This can be demonstrated by inserting realistic, or even very generous, values of body sizes, jump velocities, and hydrodynamic sensitivities in available models of hydrodynamic signal generation and perception in copepods (Kjørboe and Visser 1999; Visser 2001). Also, at the low Reynolds number of the jumping female (~ 2.5), estimated

from size (width = 0.02 cm) and jump velocity (2.5 cm s^{-1}), viscosity almost instantaneously dampens any hydrodynamic signal. This is inconsistent with the males being capable of picking up female signals that are up to 43 s old. Chemical signals, on the other hand, diffuse 1,000 times slower than momentum and, thus, persist for much longer.

Chemical signaling in the context of mate finding has been demonstrated in many other copepods (Katona 1973; Griffiths and Frost 1976), and simple models have recently been developed to describe the different extension of chemical signals related to the various motility behaviors and feeding-current characteristics typical of females of different species (Yen et al. 1998; Bagøien and Kjørboe

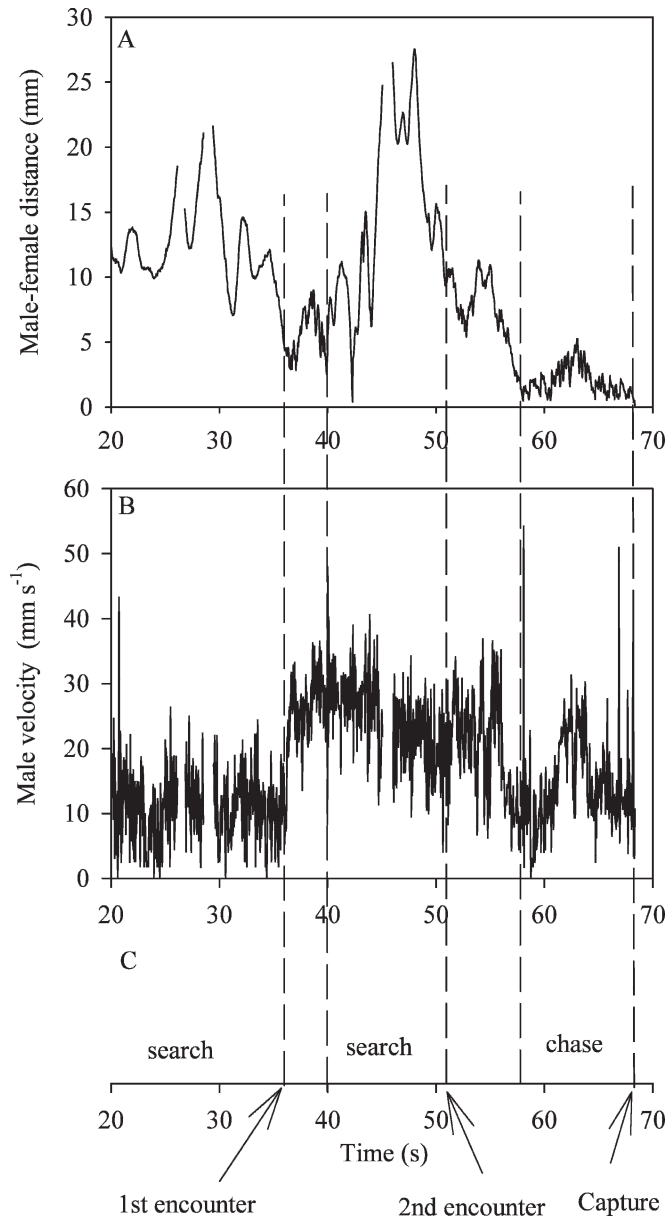


Fig. 6. Time course of (A) the distance between the mates and (B) male swimming velocity for the same mate encounter event as illustrated in Fig. 5. (C) Various sequences and events are indicated.

2005; Thygesen and Kiørboe 2006). One model that may be used as a first approximation to describe the extension of the pheromone signal in *O. davisae* considers the female as a moving point source of pheromones and results in a narrow chemical scent trail left behind the moving female. According to this model (Bagoien and Kiørboe 2005), the concentration of pheromones (C) in the immediate center of the trail varies with the along-trail distance (z) to the female as

$$C = \frac{Q}{4\pi Dz}, \quad (1)$$

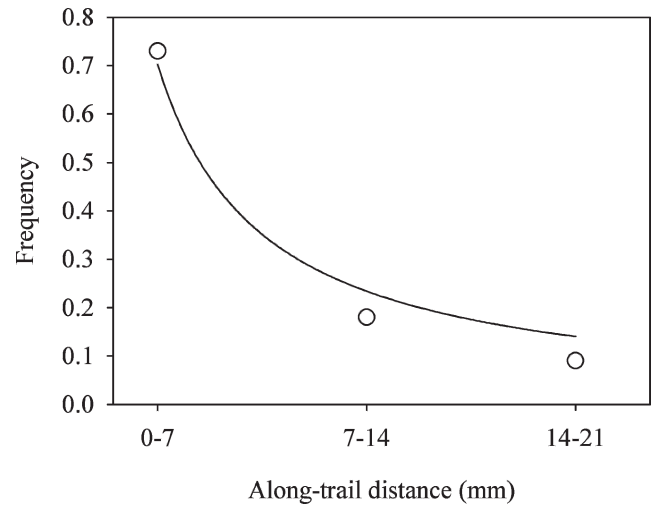


Fig. 7. *O. davisae* frequency of mate encounters as a function of the along-trail distance (L) to the female. Binned data from Table 1 ($n = 11$) and a hyperbolic model were fitted to the data, frequency = $2.5(\pm 0.2)/L$, $R^2 = 0.97$.

where Q is the release rate of pheromones, and D is the diffusion coefficient of the pheromone. The length of the detectable trail (L) is

$$L = \frac{Q}{4\pi DC^*}, \quad (2)$$

where C^* is the threshold concentration of pheromones for detection. This description of the extension of the pheromone signal is consistent with the observations in two ways. Firstly, Eq. 1 predicts that pheromone concentration varies inversely with along-trail distance to the female, consistent with the inverse relation between response frequency and along-trail distance (Fig. 7). Secondly, the ratio of pheromone-release rate over the threshold concentration for detection, Q/C^* , that can be estimated from Eq. 2 and a maximum trail length of 2 cm (Table 1) (assuming $D = 10^{-5} \text{ cm}^2 \text{ s}^{-1}$) make the observations for *O. davisae* consistent with observations for other species of cruising pelagic copepods (Fig. 9A).

The behavior of *O. davisae* males subsequent to signal detection is, however, different from that observed in other species where the female produces a pheromone trail (*Temora longicornis*, Doall et al. 1998; *Calanus marshallae*, Tsuda and Miller 1998; *Centropages typicus*, Bagoien and Kiørboe 2005). In these other species, the male, upon encountering the signal, very clearly swims up the trail while constantly checking its borders and reaches the female within seconds. *O. davisae* males, in contrast, rather swim around the trail and may spend several tens of seconds to actually locate and attack the female. During the pursuit, the male often appears to lose the trail. I interpret this as if the trail is intermittent due to the occasional jumps of the female, more like a dashed line. With jump distances of up to 1 mm, molecular diffusion cannot close the gaps fast enough to make the trail coherent; the timescale for diffusion over a distance of 1 mm is several minutes. Thus,

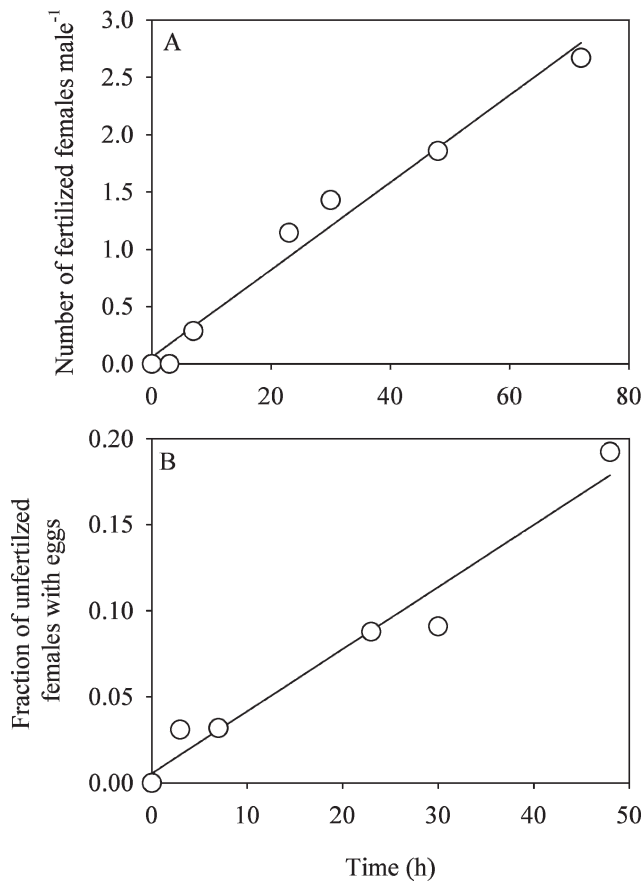


Fig. 8. (A) Mating capacity of *O. davisae* males, quantified as the cumulative number of females that are fertilized per male, and (B) the fraction of unfertilized females that carry eggs as a function of time. The fitted linear regressions are (panel A): $y = 0.061 + 0.038x$, and (panel B): $y = 5.5 \times 10^{-3} + 3.6 \times 10^{-3}x$.

the male cannot strictly follow the trail to locate the female as this ends blindly. Rather, when encountering a scent signal, he should search around it to find subsequent patches and, eventually, the female. This is apparently what he does. At the very fast tracking speed of the male, scent patches and spaces between patches, both on the order of 1 mm, are traversed in a few tenths of a millisecond, and a very fast response to variation in signal strength is therefore required for an adequate response. This is consistent with the very fast (<10 ms) motor responses to environmental stimuli that have been reported for pelagic copepods (Lenz et al. 2000).

Because the trail is intermittent, Eqs. 1 and 2 are not quite accurate descriptions of it. The trail becomes longer if one includes the dead parts. From jump distance, jump frequency, and trail age at point of detection, one can estimate the fraction of the trail which is dead and, hence, the length of the equivalent coherent trail (Table 1). The length of the equivalent coherent trail is $\sim 25\%$ shorter than the total length of the dashed trail. The revised length estimate also leads to a slightly revised estimate of the ratio of pheromone release rate over the threshold concentration for detection, $Q/C^* = 1.95 \times 10^{-4} \text{ cm}^3 \text{ s}^{-1}$ (Fig. 9).

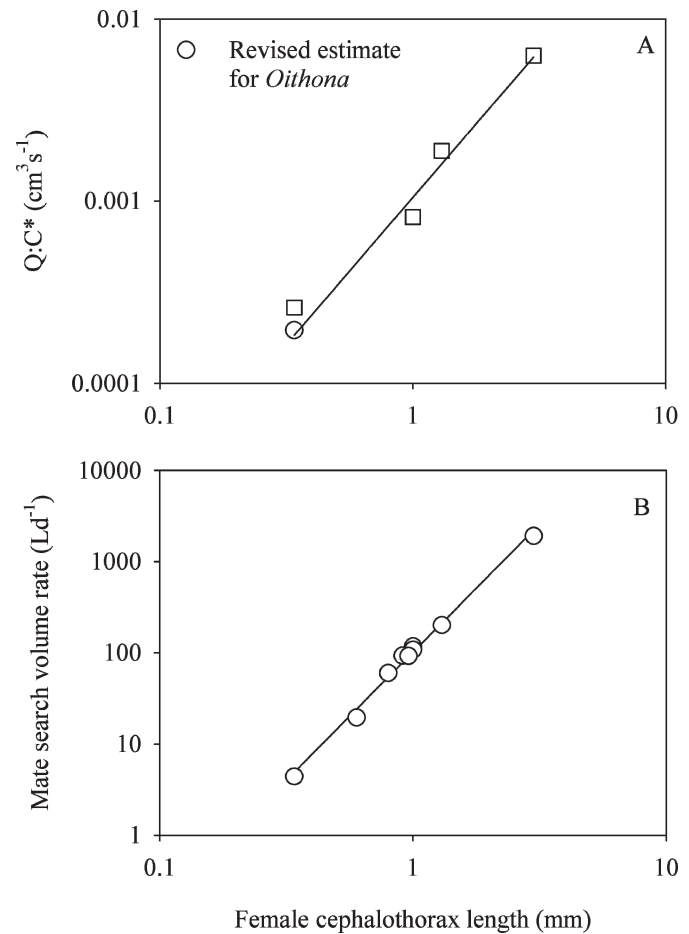


Fig. 9. (A) Scaling of the ratio of pheromone release rate to threshold concentration for detection ($Q:C^*$) with female size in four species of copepods producing pheromone mating trails. The ratio has been estimated from estimates of maximum lengths of pheromone trails using Eq. 2 and assuming a pheromone diffusivity of $10^{-5} \text{ cm}^2 \text{ s}^{-1}$. From smallest to largest copepod, the data refer to *O. davisae* (Table 1), *Temora longicornis* (Doall et al. 1998), *Centropages typicus* (Bagoien and Kjørboe 2005), and *Calanus marshallae* (Tsuda and Miller 1998). The fitted regression is: $\log(Q:C^* [\text{cm}^{-3} \text{ s}^{-1}]) = -3.0 + 1.6 \log(\text{female cephalothorax length [mm]})$. The regression uses the revised estimate for *O. davisae*. (B) Scaling of mate-search volume rate with female size for nine species of copepods employing different mate-search strategies. The smallest copepod refers to *O. davisae*, while all other data are from Kjørboe and Bagoien (2005). The fitted regression is $\log(\text{search-volume rate [L d}^{-1}]) = 2.0 + 2.8 \log(\text{female cephalothorax length [mm]})$.

While the pheromone trails of *O. davisae* and other pelagic copepods disappear due to diffusion at timescales of a few minutes, one may ask whether the continuous release of pheromones by females may lead to the buildup of a high background concentration, in the experimental aquariums or in nature, that makes pheromone signaling useless. In the absence of pheromone degradation, the time required to reach a background concentration that equals the response-threshold concentration is $(C^*/Q)/A_Q$, where A_Q is the concentration of females. In the experimental aquariums ($A_Q = 0.04 \text{ cm}^{-3}$), this time equals 36 h, more

than 10 times the incubation time, so background concentrations remain insignificant. In the ocean, however, incubation times are almost infinite and female concentrations can be even higher than in the experimental aquariums. Pheromones are likely small molecules (Bågøien and Kiørboe 2005) that probably are degraded by bacteria very fast. It requires a specific degradation rate $>(Q/C^*) \times A_0$ to keep background concentration less than the response threshold. At the highest concentration of *O. davisae* females reported by Uye and Sano (1998), 0.25 cm^{-3} , this corresponds to 4 d^{-1} , or a turnover time of 0.25 d. While such short turnover times of small molecules have been reported (Williams 2000), these considerations suggest that pheromone signaling becomes inefficient at the highest female densities of small copepods. In larger species, this problem attenuates since copepod concentration declines faster with body size (scales approximately with length^{-3}) than Q/C^* increases (scales with $\text{length}^{1.6}$; Fig. 9A).

Mate search capacity—The swimming pattern of the *O. davisae* male implies that the motility length scale (6.5 mm) exceeds the size of his target (width of female signal), which maximizes the female encounter rate. Also, the male swims very fast and actually holds a world record in sustained specific swimming velocity among copepods; a swimming velocity of 50 body lengths s^{-1} during searching and up to >100 body lengths s^{-1} during pursuit as observed in *O. davisae* males is almost an order of magnitude higher than the highest sustained swimming velocities hitherto reported for copepods (Mauchline 1998). The high swimming velocity of the males may be considered a compensation for the time spent for stationary feeding; other male copepods either don't feed or feed while swimming.

The volume of water that a male can search per unit time for female trails (β) can be estimated by (Kiørboe and Bågøien 2005):

$$\beta = 2Lu \left(\sqrt{\frac{DL}{v}} + 0.5S \right), \quad (3)$$

where L is the (corrected) maximum trail length (1.59 cm), u is the 2D average swimming velocity of the male (0.79 cm s^{-1}), v is the average 3D movement velocity of the female (0.06 cm s^{-1}), and S is the antennal span of the male (0.04 cm). Inserting the respective values yields a search-volume rate of 4.4 L d^{-1} , which makes *O. davisae* in line with all previous estimates for pelagic copepods, whether they use hydrodynamic or chemical signaling, and independent of the character of the chemical signal of the female and of the motility pattern of the male (Fig. 9B).

Mating capacity—The males of *O. davisae* have a surprisingly low capacity to fertilize females, less than one successful mating per male per day, even when encounter rates are nonlimiting. The males of many calanoid copepods don't feed after maturation, and these males, obviously, have a finite number of spermatophores. The actual numbers are quite uncertain, however; Hopkins

(1978) estimated a potential lifetime output of about three spermatophores in *Euchaeta norvegica*, whereas Mauchline (1998) estimated ~ 10 – 100 spermatophores for a range of species based on a somewhat arbitrary assumption that a male would produce spermatophores corresponding to 10% of his body mass. Males of other copepods do feed, as do the males of *O. davisae* (own unpubl. data), and one would expect a spermatophore production capacity of the same order as egg-production rates in the females, particularly in *O. davisae*, where the spermatophores are much smaller than the eggs ($25 \mu\text{m}$ vs. $60 \mu\text{m}$). However, the only other direct estimate of spermatophore production rate in a pelagic copepod is for *Temora stylifera*, and it is similar to the mating capacity reported here for *O. davisae*, 0.4 – 1.4 spermatophores $\text{male}^{-1} \text{ d}^{-1}$ (Ianora and Poulet 1993; Ianora et al. 1999).

Population dynamics—The recruitment to a population of copepods depends on the potential egg-production rate as well as on the fraction of females that have been fertilized. If the latter is low, recruitment is low. In *O. davisae*, the female needs to be mated only once to remain fertile during the rest of its adult life (Uchima 1985). The fraction of fertilized females (σ) in a population depends on the males' mate-search volume rate (β), on their mating capacity (α), on the mortality rate of the females (δ), on the density of adults (A), and on the male-to-female ratio (π) as follows (Kiørboe 2006):

$$\sigma = \frac{\beta A}{\delta + \beta A + (\delta + \delta \beta A / \alpha) / \pi}. \quad (4)$$

Uye and Sano (1995, 1998) reported the seasonal variation in the fraction of breeding females and in adult male and female densities of *O. davisae* in a eutrophic inlet in the Inland Sea of Japan (Fig. 10A–C). Using the reported adult densities, an estimated mortality rate of 0.2 d^{-1} as a typical value for copepods of the size of *O. davisae* (Hirst and Kiørboe 2002), and the above estimates of mating and mate-search capacity, we can find the seasonal variation in the fraction of fertilized females (Fig. 10C). A comparison of observed and predicted patterns reveals first that the seasonal averages of the predicted and observed fractions of fertilized breeding females, respectively, are similarly low, approximately one-third of the females (0.39 ± 0.34 vs. 0.36 ± 0.33), and secondly that the seasonal trends are similar. The temporal correlation between observed and predicted fraction fertilized is relatively low, but highly significant ($r = 0.39$, $p < 0.001$). This suggests that the low fraction of breeding females is in fact due to fertilization limitation. Food shortage might also result in a low fraction of the females not carrying eggs, but food was probably rarely limiting in the study area, as judged from high chlorophyll concentrations, $\sim 5 \mu\text{g L}^{-1}$, when the fraction of breeding females was at its lowest. Also, during November–June, the specific egg-production rate was a linear function of temperature and independent of variation in food concentration, again suggesting that food was not limiting reproduction (Uye

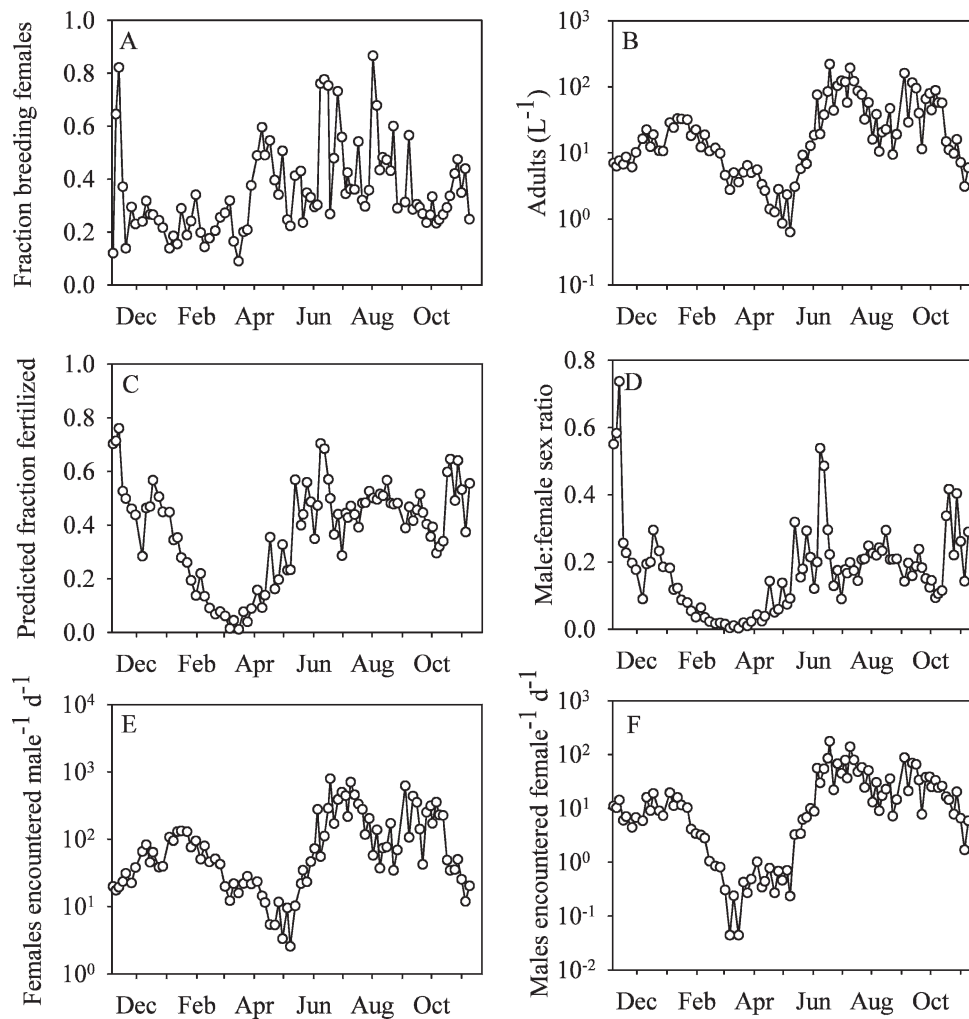


Fig. 10. Seasonal variation in population characteristics and abundances of *O. davisae* in Fukuyama Harbor, Inland Sea of Japan. (A) Observed fraction of breeding females, (B) adult concentration, (C) predicted fraction of fertilized females, (D) male:female sex ratio, and (E) male or (F) female mate-encounter rates. Data in panels A, B, and D are from the field observations of Uye and Sano (1995, 1998). Uye and Sano (1995) estimated the fraction of breeding females from the fraction carrying eggs by taking the temperature-dependent duration of the interclutch period into account. The data in panels C, E, and F have been computed or modeled from field and laboratory data. Male and female encounter rates are computed as mate-encounter search volume (4.4 L d^{-1}) multiplied by field-observed female and male concentrations, respectively.

and Sano 1995). The computed fraction of fertilized females apparently underpredicts the fraction of breeding females during winter. This may be due to a lower than average mortality of *O. davisae* during late winter, such as has been observed for other *Oithona* species (Eiane and Ohman 2004), as this will increase the fraction of fertilized females (cf. Eq. 4). It may also be caused by unfertilized females producing eggs (cf. Fig. 8B), in which case fertilization limitation is even more severe than the observations would suggest. In either case, both observations and model predictions suggest that population growth is severely limited by fertilization limitation throughout the year and potentially mostly so during late winter.

Mating rate may be limited by mate-encounter rate and/or by the mating capacity of the males. The rate at which females encountered males in the study area of Uye and Sano (1995, 1998) was $>10 \text{ males d}^{-1}$ for most of the year (Fig. 10E). Only during late winter did this fall to $0.1\text{--}1.0$ encounters d^{-1} . With an average longevity of 5 d (follows from a mortality of 0.2 d^{-1}), some females never meet a male, and fertilization rate would thus be limited by mate-encounter rate. During the remainder of the year, mating is not limited by encounter rate. However, throughout the year, males meet females at a rate $\gg 1\text{--}1,000 \text{ d}^{-1}$ (Fig. 10F), i.e., many more than they can mate. Male mating capacity, or the abundance of males, thus constant-

ly limits fertilization rate and, therefore constrains the population growth rate.

The simple theoretical model used here to connect individual behaviors to population processes does not pretend to be very accurate in its predictions because it does not include all relevant processes and because all parameters are not equally well determined. However, the conclusion that the population is fertilization limited due to male mating capacity is quite robust to variations in the estimates of mating capacity (α), mate-search capability (β), and mortality (δ), the three parameters upon which the fraction of fertilized females depends (Eq. 4). Changing β by an order of magnitude alters the predicted average fraction of fertilized females by less than 0.04. This fraction is, of course, more sensitive to inaccuracies in α , but even a doubling of the mating capacity leads only to about half the females being fertilized on average ($\sigma = 0.54$), and it takes a 10 times increase in mating capacity to reach 80% predicted fertilized. High adult mortalities, rather than a limited mating capacity, could in principle also account for the low fraction of breeding females in the field population, but it would require a doubling of the mortality rate (to an unreasonable 0.4 d^{-1}) to compensate for a doubling of the mating capacity. Finally, environmental factors, such as food shortage, would tend to decrease rather than increase the mating capacity of the males compared to that observed at food saturation in the laboratory.

In an evolutionary context, it is surprising that the neritic *O. davisae*, which typically occurs in very high abundances in estuaries and inlets (Nishida 1985; Hirota 1990; Fig. 10), has developed such strong mate-searching skills and such poor mating capacity. Such a strategy would appear well suited for oceanic conditions where abundances are low and mate encounters, rather than spermatophore production, become critical. One may speculate that such a strategy may be reminiscent from a more oceanic ancestor or represent an adaptation to periods where population density is low.

In conclusion, behavioral and field observations together with population models suggest that *O. davisae* population growth is severely limited by fertilization rate and by a shortage of males, even when population densities are high, mainly because the males have a limiting capacity to produce spermatophores and because the sex ratio of the field population is severely female biased. Because sex ratios have to be close to 1 : 1 at birth (Fisher 1930), and remain so at the time of maturation in laboratory cultures of *O. davisae* (own unpubl. data), the biased sex ratio in the field population is caused by a higher male than female mortality rate. The higher mortality of males may partly be caused by their mate-searching behavior, which not only increases the rate of female encounter but also the risk of meeting a predator. One may ask how common fertilization limitation is among populations of pelagic copepods. Kiørboe (2006) argued that fertilization limitation would be pronounced when population densities are close to the lower threshold for population maintenance and showed for several temperate species that such population densities typically occur during late winter. If the limited mating capacity reported for *O. davisae* and a few other species applies more generally, then fertilization limitation could be

important also during peak seasons. This would in particular apply to species where the females require frequent remating to stay fertile (e.g., members of the superfamily Centropagoidea; Ohtsuka and Huys 2001), and to species with very female-biased population sex ratios (such as the Oithonidae, Euchaetida, and Calanidae families; Kiørboe 2006). As demonstrated here, it takes a substantial increase in mating capacity to reach something near 100% fertilization frequency. Fertilization limitation may thus partly account for the frequent observations of low hatching success of copepod eggs in field studies.

References

- BAGØIEN, E., AND T. KIØRBOE. 2005. Blind dating—mate finding in planktonic copepods. I. Tracking the pheromone trail of *Centropages typicus*. *Mar. Ecol. Prog. Ser.* **300**: 105–115.
- BAN, S., AND OTHERS. 1997. The paradox of diatom-copepod interactions. *Mar. Ecol. Prog. Ser.* **157**: 287–293.
- CALBET, A., AND S. AGUSTI. 1999. Latitudinal changes of copepod egg production rates in Atlantic waters: Temperature and food availability as the main driving factors. *Mar. Ecol. Prog. Ser.* **181**: 155–162.
- CASTELLANI, C., AND I. A. N. LUCAS. 2003. Seasonal variation in egg morphology and hatching success in the calanoid copepods *Temora longicornis*, *Acartia clausi* and *Centropages hamatus*. *J. Plankton Res.* **25**: 527–537.
- DOALL, M. H., S. P. COLIN, J. R. STRICKLER, AND J. YEN. 1998. Locating a mate in 3D: The case of *Temora longicornis*. *Phil. Trans. R. Soc. Lond. B* **353**: 681–689.
- EIANE, K., AND M. D. OHMAN. 2004. Stage-specific mortality of *Calanus finmarchicus*, *Pseudocalanus elongatus* and *Oithona similis* on Fladen Ground, North Sea, during a spring bloom. *Mar. Ecol. Prog. Ser.* **268**: 183–193.
- FISHER, R. A. 1930. The genetical theory of natural selection. Oxford Univ. Press.
- GRIFFITHS, A. M., AND B. W. FROST. 1976. Chemical communication in the marine planktonic copepods *Calanus pacificus* and *Pseudocalanus* sp. *Crustaceana* **30**: 1–9.
- HIROTA, R. 1990. Microdistribution of the marine copepod *Oithona davisae* in the shallow waters of Ariake-kai mud flats, Japan. *Mar. Biol.* **105**: 307–312.
- HIRST, A. G., AND T. KIØRBOE. 2002. Mortality of marine planktonic copepods: Global rates and patterns. *Mar. Ecol. Prog. Ser.* **230**: 195–209.
- HOPKINS, C. C. E. 1978. The male genital system, and spermatophore production and function in *Euchaeta norvegica* Boeck (Copepoda: Calanoida). *J. Exp. Mar. Biol. Ecol.* **35**: 197–231.
- . 1982. The breeding biology of *Euchaeta norvegica* (Boeck) (Copepoda, Calanoida) in Loch Etive, Scotland—assessment of breeding intensity in terms of seasonal cycles in the sex-ratio, spermatophore attachment, and egg-sac production. *J. Exp. Mar. Biol. Ecol.* **60**: 91–102.
- IANORA, A., AND S. A. POULET. 1993. Egg viability in the copepod *Temora stylifera*. *Limnol. Oceanogr.* **38**: 1615–1626.
- , A. MIRALTO, I. BUTTINO, AND G. ROMANO. 1999. First evidence of some dinoflagellates reducing male copepod fertilization capacity. *Limnol. Oceanogr.* **44**: 147–153.
- , B. SCOTTO DI CARLO, AND P. MASCELLARO. 1989. Reproductive biology of the planktonic copepod *Temora stylifera*. *Mar. Biol.* **101**: 187–194.
- IRIGOIEN, X., AND OTHERS. 2002. Copepod hatching success in marine ecosystems with high diatom concentrations. *Nature* **418**: 387–389.

- KATONA, S. 1973. Evidence for sex pheromones in planktonic copepods. *Limnol. Oceanogr.* **18**: 574–583.
- KJØRBOE, T. 2006. Sex, sex-ratios, and the dynamics of pelagic copepod populations. *Oecologia* **148**: 40–50.
- , AND E. BAGØIEN. 2005. Motility patterns and mate encounter rates in planktonic copepods. *Limnol. Oceanogr.* **50**: 1999–2007.
- , AND A. W. VISSER. 1999. Predator and prey perception in copepods due to hydromechanical signals. *Mar. Ecol. Prog. Ser.* **179**: 81–95.
- LENZ, P. H., D. K. HARLINE, AND A. D. DAVIES. 2000. The need for speed. I. Fast reactions and myelinated axons in copepods. *J. Comp. Physiol. A* **186**: 337–345.
- MAPS, F., J. A. RUNGE, B. ZAKARDJIAN, AND P. JOLY. 2005. Egg production and hatching success of *Temora longicornis* (Copepoda, Calanoida) in the southern Gulf of St. Lawrence. *Mar. Ecol. Prog. Ser.* **285**: 117–128.
- MAUCLINE, J. 1998. The biology of calanoid copepods. *Adv. Mar. Biol.* **33**: 1–710.
- MIRALTO, A., AND OTHERS. 1999. The insidious effect of diatoms on copepod reproduction. *Nature* **402**: 173–176.
- NISHIDA, S. 1985. Taxonomy and distribution of the family oithonidae (Copepoda, Cyclopoida) in the Pacific and Indian Oceans. *Bull. Ocean Res. Inst. Univ. Tokyo* **20**: 1–167.
- OHTSUKA, S., AND R. HUYS. 2001. Sexual dimorphism in calanoid copepods: Morphology and function. *Hydrobiologia* **453/454**: 441–466.
- PARRISH, K. K., AND D. F. WILSON. 1978. Fecundity studies on *Acartia tonsa* (Copepoda: Calanoida) in standardized cultures. *Mar. Biol.* **46**: 65–81.
- PETERSON, W. T., P. TISELIUS, AND T. KJØRBOE. 1991. Copepod egg-production, molting and growth rates, and secondary production in the Skagerrak in August 1988. *J. Plankton Res.* **13**: 131–154.
- THYGESEN, U. H., AND T. KJØRBOE. 2006. The diffusive transport in a Stokeslet and its application to plankton ecology. *J. Math. Biol.* **53**: 1–14.
- TSUDA, A., AND C. B. MILLER. 1998. Mate-finding behaviour in *Calanus marshallae* Frost. *Phil. Trans. R. Soc. Lond. B* **353**: 713–720.
- UCHIMA, M. 1985. Copulation in the marine copepod *Oithona davisae* Ferrari and Orsi. *Bull. Plankton Soc. Japan* **32**: 31–36.
- , AND R. HIRANO. 1988. Swimming behaviour of the marine copepod *Oithona davisae*: Internal control and search for environment. *Mar. Biol.* **99**: 47–56.
- , AND M. MURANO. 1988. Mating behaviour of the marine copepod *Oithona davisae*. *Mar. Biol.* **99**: 39–45.
- UYE, S., AND K. SANO. 1995. Seasonal reproductive biology of the small cyclopoid copepod *Oithona davisae* in a temperate eutrophic inlet. *Mar. Ecol. Prog. Ser.* **118**: 121–128.
- , AND K. SANO. 1998. Seasonal variations in biomass, growth rate and production rate of the small cyclopoid copepod *Oithona davisae* in a temperate eutrophic inlet. *Mar. Ecol. Prog. Ser.* **163**: 37–44.
- VISSER, A. W. 2001. Hydromechanical signals in the plankton. *Mar. Ecol. Prog. Ser.* **222**: 1–24.
- , AND T. KJØRBOE. 2006. Plankton motility patterns and encounter rates. *Oecologia* **148**: 538–546.
- WILLIAMS, P. J. LE.B. 2000. Heterotrophic bacteria and the dynamics of dissolved organic material, p. 153–200. *In* D. L. Kirchman [ed.], *Microbial ecology of the ocean*. Wiley-Liss, Inc.
- WILLIAMSON, C. E., AND N. M. BUTLER. 1987. Temperature, food and mate limitation of copepod reproductive rates: Separating the effects of multiple hypotheses. *J. Plankton Res.* **9**: 821–836.
- YEN, J., M. J. WEISSBURG, AND M. H. DOALL. 1998. The fluid physics of signal perception by mate-tracking copepods. *Phil. Trans. R. Soc. Lond. B* **353**: 787–804.

Received: 19 September 2006

Accepted: 28 February 2007

Amended: 14 March 2007